AJNR

Diffusion-tensor MR Imaging of the Human Brain with Gradient- and Spin-echo Readout: Technical Note

Ryuta Itoh, Elias R. Melhem and Paul J.M. Folkers

AJNR Am J Neuroradiol 2000, 21 (9) 1591-1595
http://www.ajnr.org/content/21/9/1591

AJNR Am J Neuroradiol 21:1591–1595, October 2000

Technical Note

Diffusion-tensor MR Imaging of the Human Brain with Gradient- and Spin-echo Readout: Technical Note

Ryuta Itoh, Elias R. Melhem, and Paul J.M. Folkers

Summary: Diffusion-tensor MR imaging of the brain is an objective method that can measure diffusion of water in tissue noninvasively. Five adult volunteers participated in this study that was performed to evaluate the potential of gradient- and spin-echo readout for diffusion-tensor imaging by comparing it with single-shot spin-echo echo-planar imaging. Gradient- and spin-echo readout provides comparable measures of water diffusion to single-shot spin-echo echo-planar readout with significantly less geometrical distortion at the expense of a longer imaging time.

Diffusion-tensor MR imaging of the brain has been proposed as a noninvasive technique that provides microstructural and physiological information regarding brain tissue in vivo by measuring the diffusion of water (1, 2). Most current applications of diffusion-tensor MR imaging implement ultrafast single-shot echo-planar readouts, which effectively freeze physiological effects (3–5) despite severe geometrical distortions caused by local magnetic field inhomogeneity. Gradient- and spin-echo (GRASE) MR imaging has less distortion compared with single-shot echo-planar imaging because the multiple refocusing RF pulses implemented in GRASE MR imaging are responsible for reducing errors originating from static field inhomogeneity (6). For this technical note, we compared the signal-to-noise ratio (SNR), isotropic apparent diffusion coefficient (ADCi), fractional anisotropy (FA), and geometrical distortions from diffusion-tensor MR imaging by use of GRASE and echo-planar readout techniques.

Description of the Technique

MR Imaging and Data Processing

MR imaging studies were performed on a 1.5-T MR system (ACS-NT; Philips Medical Systems, Best, The Netherlands) using a quadrature head coil operating in receive mode. The whole-brain MR imaging protocol included axial T1-weighted spin-echo 517/14/2 (TR/TE/excitations) imaging and axial diffusion-tensor imaging using peripheral gating. The diffusion tensor MR imaging was performed using single-shot spin-echo echo-planar and GRASE readouts. Diffusion sensitization was applied sequentially in six different non-colinear directions (G_{xx}, G_{yy}, G_{zz}, G_{xy}, G_{xz}, G_{yz}). The parameters for single-shot spin-echo echo-planar diffusion-tensor imaging were 3429–5538/96/4 (TR/effective TE/excitations), with a b value of 600 $s \cdot mm^{-2}$. The parameters for GRASE diffusion-tensor imaging with four spin echoes each comprising five gradient echoes were 4000–4615/119 (TR/TE_{eff}), with a b value of 600 $s \cdot mm^{-2}$. To eliminate phase errors that originated during the diffusion preparation period, a dephasing gradient and a 90-degree RF pulse before the GRASE readout were used (7). The T1-weighted spin-echo sequence and both the diffusion-tensor sequences were matched for total brain coverage (number of sections, 18; section thickness, 5 mm; intersection gap, 1 mm; field of view, 23 cm). The GRASE experiment was performed twice, once with four excitations (4-GRASE) and once with 10 excitations (10-GRASE). The matrices and acquisition times (minutes:seconds) of single-shot spin-echo echo-planar, 4-GRASE, and 10-GRASE imaging were 128 × 95 (2:46–3:26), 128 × 100 (9:32–11:00), and 128 × 80 (14:12–15:59), respectively.

The six independent elements of the diffusion tensor (Dxx, Dyy, Dzz, Dxy, Dxz, Dyz) were calculated using multivariate linear regression (1) in each voxel by an imager built-in research application program. From the diffusion-tensor data, voxel-by-voxel brain maps of the ADCi ([ADCxx + ADCyy + ADCzz]/3) and FA (8) were generated on-line by standard matrix procedures.

Five healthy adult volunteers (average age, 33.6 years; male: female ratio, 4:1) underwent imaging. The human participant protocol was approved by the institutional internal review board, and informed consent was obtained from all participating volunteers.

Analysis of SNR, FA, and ADCi

Non-diffusion-weighted images (b_0 images [Fig 1A and B]), ADCi, and FA (Figs 2 and 3) maps were transferred to a workstation equipped with commercially available software. Measurements were made by using variably sized oval-shaped regions of interest manually placed in the putamen, the corpus callosum, and the centrum semiovale.

SNR

The mean signal intensities within the regions of interest on the b_0 images were measured. The SD of the mean signal intensity of background areas outside the head was used to estimate noise. Ranges of average SNRs (SDs) of the locations for single-shot spin-echo echo-planar, 4-GRASE, and 10-GRASE were 52.4–64.0 (4.4–11.5), 22.4–26.5 (1.5–4.5), and 38.2–40.2 (3.2–4.1), respectively. Single-shot spin-echo echo-planar MR imaging provided images of the brain with significantly better SNR than did 4-GRASE and 10-GRASE (*t* test, $P < .01$ and $P < .05$, respectively).

Received February 1, 2000; accepted after revision May 3.

From the Department of Radiology and Radiological Sciences (R.I., E.R.M.), The Johns Hopkins Medical Institutions, Baltimore, MD, and the Philips Medical System (P.J.M.F.), Best, The Netherlands.

This work was conducted at the F.M. Kirby Research Center for Functional Brain Imaging.

Address reprint requests to Elias R. Melhem, MD, Department of Radiology, The Johns Hopkins Hospital, 600 North Wolfe Street, Baltimore, MD 21287–2182.

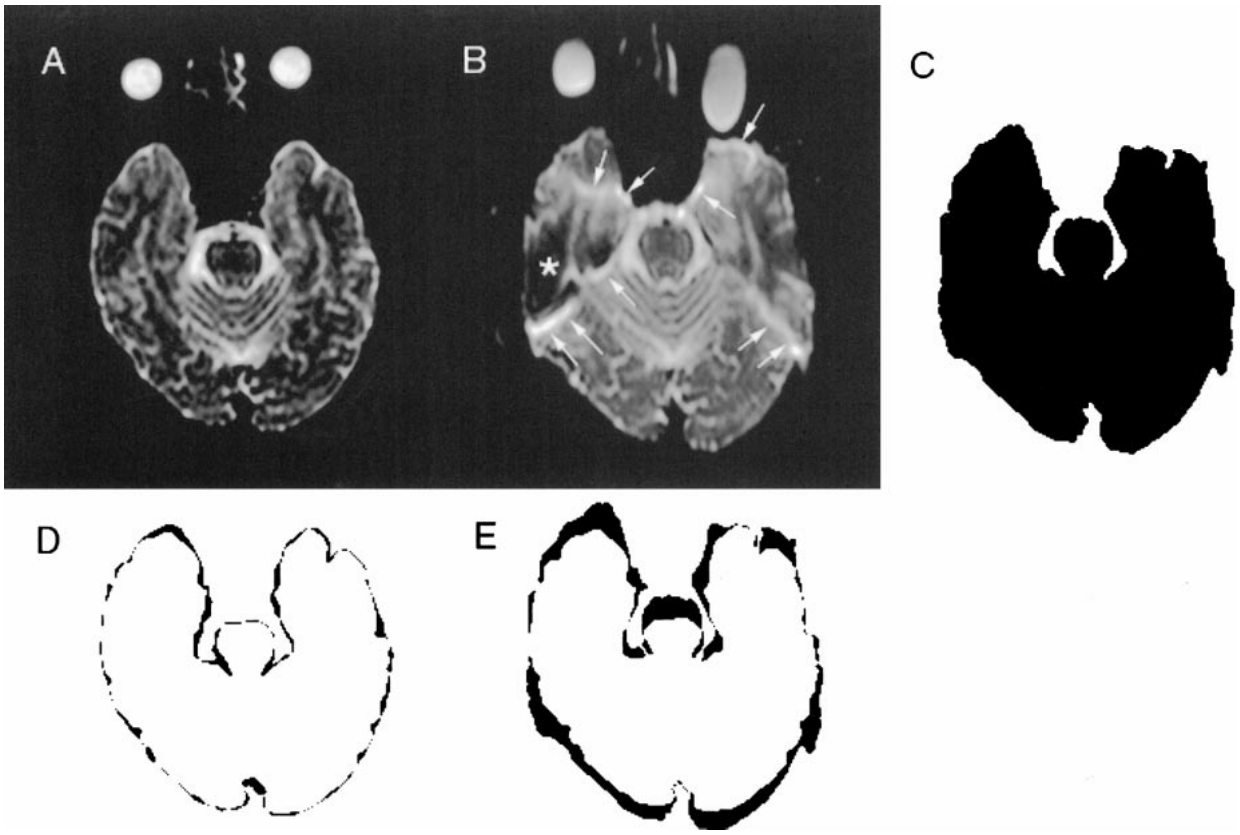

FIG 1. Images of a 35-year-old male volunteer.

A, Axial 4-GRASE b_0 image, 4615/119/4 (TR/TE_{eff}/excitations), obtained at the level of the temporal lobe base.

B, Single-shot spin-echo echo-planar b_0 image, 5538/96/4, obtained at the level of the temporal lobe base.

C, Thresholded binary image generated from single-shot spin-echo echo-planar b_0 image.

D, Difference image obtained by subtracting the binary maps of the 4-GRASE b_0 images from the binary map of the T1-weighted spin-echo image.

E, Difference image obtained by subtracting the binary maps of the single-shot spin-echo echo-planar b_0 images from the binary map of the T1-weighted spin-echo image. Note that the distortion index (number of pixels in the black zone) is greater for the subtracted image *E* than *D,* which is the result of more severe distortion in the single-shot spin-echo echo-planar b_0 images, as shown by thick bands of signal loss (*) and signal hyperintensity (*arrows*).

ADCi and FA

The averages and SDs of ADCi and FA values for the different anatomic locations are reported in the Table. There was no significant difference in average FA and ADCi values for all anatomic locations between single-shot spin-echo echo-planar and 10-GRASE imaging (*t* test, $P > .05$). When comparing 4-GRASE and 10-GRASE diffusion-tensor imaging, a significant difference is found in the average FA for the right putamen and right centrum semiovale (*t* test, $P < .05$) and in the average ADCi for the right putamen only (*t* test, $P < .05$) (Fig 3).

Estimation of Distortion

T1-weighted images and original diffusion-tensor images of single-shot spin-echo echo-planar and 4-GRASE techniques were transferred to a personal computer equipped with an image-processing application (NIH Image 1.61). Threshold binary maps (Fig 1C) were obtained by manually setting the threshold and automatically tracing the outline of the brain. Next, the difference images were calculated by subtracting the binary maps on a pixel-by-pixel basis (Figs 1D and E). The total number of pixels represented areas of mismatch between the different binary maps and constituted the distortion index.

Distortion from Static Magnetic Field Inhomogeneity

A distortion index 1 was obtained from the difference images, which were calculated by subtracting the b_0 image from the T1-weighted image. The distortion index 1 averages (pixels) (SD) of the 4-GRASE technique versus the single-shot spin-echo echo-planar technique at the level of the temporal lobe base, the frontal lobe base, and the centrum semiovale were 921.8 (61.0) versus 2381.4 (625.9), 693.6 (130.1) versus 1840.8 (605.2), and 791.4 (55.5) versus 1317.0 (365.9), respectively. The distortion index 1 averages of the 4-GRASE technique were less than those of the single-shot spin-echo echo-planar technique at all three levels (*t* test, $P < .05$). Bonferroni's multiple comparison reveals that the index 1 of the temporal lobe base of the GRASE technique was greater than that of the frontal lobe base level and also reveals that the index 1 of the temporal lobe base level of the single-shot spin-echo echo-planar technique was greater than that of the centrum semiovale level. Furthermore, the average proportion of the number of sections with severe distortions (marked signal intensity loss or peripheral high intensity band of the distorted area [Fig 1B]) to the total number of sections was 6/18 for the single-shot spin-echo echo-planar technique and 0/18 for the GRASE technique (*t* test, $P < .01$).

Eddy Current-induced Distortions by the Diffusion-sensitization Gradient

A distortion index 2 was obtained from the difference images, which were generated by subtracting each of the six-direction diffusion-weighted images from the b_0 image at the

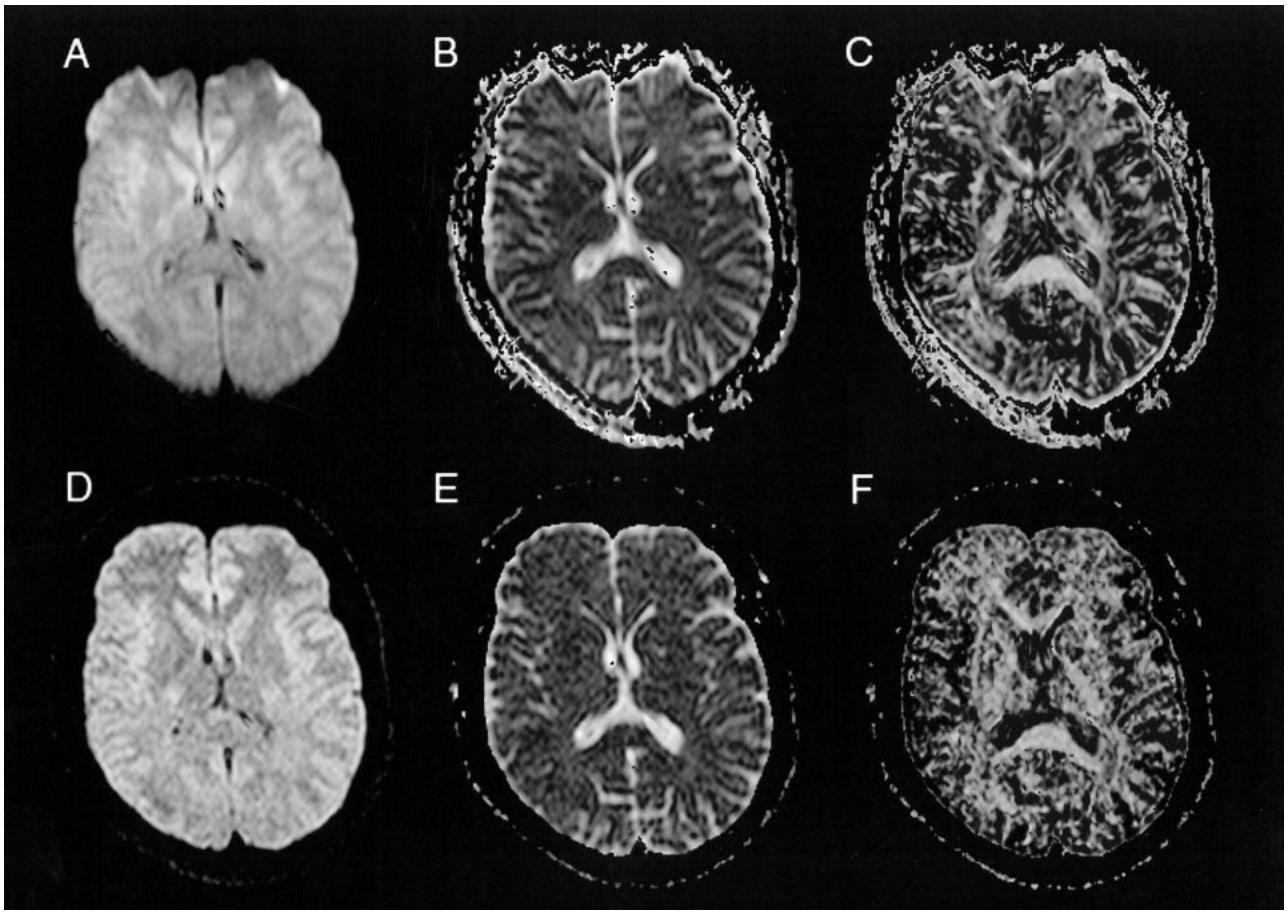

FIG 2. Images of a 34-year-old male volunteer.

A, Axial single-shot spin-echo echo-planar 3429/96/4 MR image, obtained at the level of the basal ganglia. The single-shot spin-echo echo-planar diffusion-weighted MR image and the corresponding maps (*B, C*) show a greater degree of distortion of the frontal lobes around the frontal sinuses and a higher SNR than do the 4-GRASE diffusion-weighted MR image and maps (*D, E, F*).

B, Corresponding ADCi map.

C, Corresponding FA map.

D, 4-GRASE 4286/119/4 diffusion-weighted image, obtained at the level of the basal ganglia.

E, Corresponding ADCi map.

F, Corresponding FA map.

Averages and standard deviations (SDs) of ADCi (10^{-5} mm^2/sec) and FA values for the different brain anatomic locations

Anatomic Location		SE EPI	4-GRASE	10-GRASE
Right putamen	ADCi (SD)	76.4 (6.9)	89.4 (5.1)	81.0 (1.6)
	FA (SD)	0.25 (0.03)	0.32 (0.03)	0.27 (0.02)
Left putamen	ADCi (SD)	75.6 (2.9)	83.8 (3.1)	80.6 (4.7)
	FA (SD)	0.24 (0.05)	0.31 (0.04)	0.26 (0.04)
Corpus callosum	ADCi (SD)	80.4 (10.4)	82.0 (8.2)	80.3 (5.0)
	FA (SD)	0.71 (0.02)	0.70 (0.02)	0.71 (0.06)
Right centrum semiovale	ADCi (SD)	88.0 (5.2)	92.4 (6.1)	88.5 (4.8)
	FA (SD)	0.35 (0.04)	0.42 (0.03)	0.34 (0.06)
Left centrum semiovale	ADCi (SD)	87.0 (6.6)	87.6 (6.7)	89.0 (2.0)
	FA (SD)	0.35 (0.05)	0.41 (0.03)	0.37 (0.03)

level of the centrum semiovale. The averages of the distortion index 2 of each diffusion sensitization gradient direction were calculated and were compared for the two techniques. The distortion index 2 average (pixels) of the GRASE technique (889.7) was significantly less than that of the single-shot spin-echo echo-planar technique (1038.7) (*t* test, $P < .01$).

Discussion

In diffusion-tensor MR imaging, it is important to acquire geometrical distortion-free images because misregistration caused by the distortions can affect the spatial resolution and accuracy of diffu-

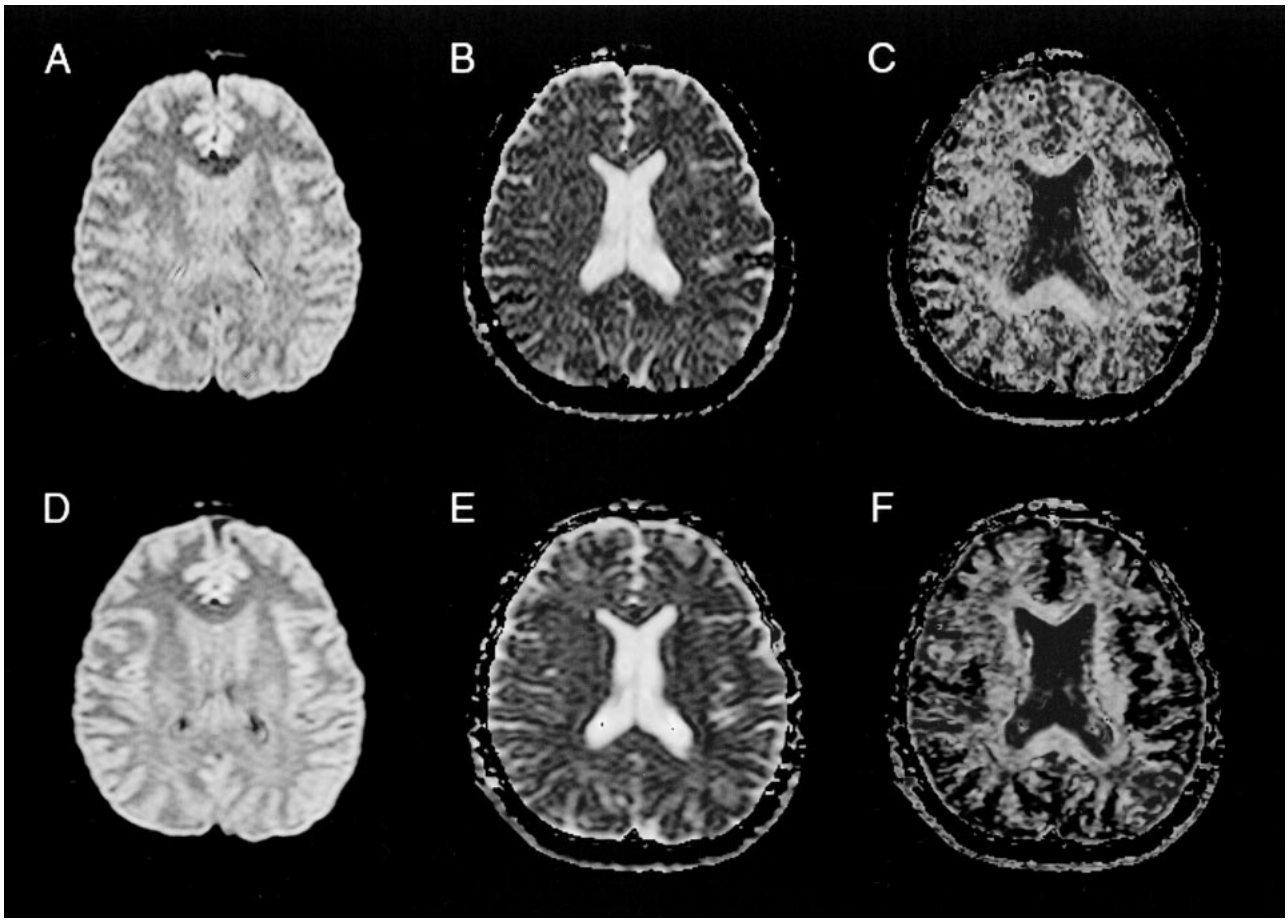

FIG 3. Images of a 34-year-old male volunteer (same volunteer as in Fig 2).
A, Axial 4-GRASE 4286/119/4 image, obtained at the level of the lateral ventricle body.
B, Corresponding ADCi map.
C, Corresponding FA map.
D, 10-GRASE 4286/119/10 diffusion-weighted MR image, obtained at the level of the lateral ventricle body. As expected, the 10-GRASE diffusion-weighted MR image and maps (*D, E, F*) show higher SNR than the 4-GRASE diffusion-weighted MR image and maps (*A, B, C*) at the expense of longer acquisition time.
E, Corresponding ADCi map.
F, Corresponding FA map.

sion and anisotropy maps calculated on a pixel-by-pixel basis (9). GRASE MR imaging is inherently resistant to the distortions due to field inhomogeneity errors, because k-space trajectory of GRASE MR imaging sweeps through multiple discontinuous and modulated paths on the phase axis (6). Therefore, GRASE MR imaging can provide almost geometrical distortion-free diffusion-tensor MR images without the need for the complex and time-consuming correction algorithms that are needed for the single-shot echo-planar technique (9–11). Our results show that GRASE diffusion-tensor MR imaging has very little distortion from static field inhomogeneities and diffusion sensitization gradient-induced eddy currents compared with single-shot spin-echo echo-planar diffusion-tensor imaging.

With our GRASE diffusion-tensor imaging, only half the original magnetization is sampled because of the dephasing gradient and the 90° RF (7). Consequently, the major disadvantage of our GRASE diffusion-tensor MR imaging is a lower SNR per acquisition time. The 10-GRASE sequence needs an approximately five times longer acquisition time (14–16 min) than does the 4-GRASE or single-shot spin-echo echo-planar sequence (3–3.5 min) to acquire enough SNR for obtaining ADCi and FA values similar to those obtained from spin-echo echo-planar diffusion-tensor imaging. Our results show that the GRASE sequence with peripheral gating can successfully acquire the physiological effect-free data when the participants are healthy adults who can keep still for 15 minutes. However, the long acquisition time increases the probability of artifact by involuntary head motions during imaging and also makes it difficult to include the imaging in a routine clinical examination.

Because of the significant reduction in geometrical distortions offered by the GRASE readout, new pulse sequence designs intended to improve SNR per acquisition time are being developed. In the future, the GRASE readout technique may be

an attractive alternative to the single-shot spin-echo echo-planar technique for diffusion-tensor MR imaging.

Acknowledgements

The authors thank the Uehara Memorial Foundation, Tokyo, Japan, for their fellowship.

References

1. Basser PJ, Mattiello J, LeBihan D. **MR diffusion tensor spectroscopy and imaging.** *Biophys J* 1994;66:259–267
2. Basser PJ, Mattiello J, LeBihan D. **Estimation of the effective self-diffusion tensor from the NMR spin echo.** *J Magn Reson B* 1994;103:247–254
3. Pierpaoli C, Jezzard P, Basser PJ, Barnett A, DiChiro G. **Diffusion tensor MR imaging of the human brain.** *Radiology* 1996;201: 637–648
4. Turner R, LeBihan D. **Single-shot diffusion imaging at 2.0 tesla.** *J Magn Reson* 1990;86:445–452
5. Turner R, LeBihan D, Maier J, Vavrek R, Hedges LK, Pekar J. **Echo-planar imaging of intravoxel incoherent motion.** *Radiology* 1990;177:407–414
6. Oshio K, Feinberg DA. **GRASE (gradient- and spin-echo) imaging: a novel fast MRI technique.** *Magn Reson Med* 1991;20: 344–349
7. Alsop DC. **Phase insensitive preparation of single-shot RARE: application to diffusion imaging in humans.** *Magn Reson Med* 1997;38:527–533
8. Basser PJ, Pierpaoli C. **Microstructural and physiological features of tissues elucidated by quantitative-diffusion-tensor MRI.** *J Magn Reson B* 1996;111:209–219
9. Jezzard P, Barnet AS, Pierpaoli C. **Characterization of and correction for eddy current artifacts in Echo Planar diffusion imaging.** *Magn Reson Med* 1998;39:801–812
10. Jezzard P, Balaban RS. **Correction for geometric distortion in echo planar images from B0 field variations.** *Magn Reson Med* 1995;34:65–73
11. Haselgrove JC, Moore JR. **Correction for distortion of echo-planar images used to calculate the apparent diffusion coefficient.** *Magn Reson Med* 1996;36:960–964